Bioconjugate Chemistry

Article

pubs.acs.org/bc

Preparation of Covalently Linked Complexes Between DNA and O^6-Alkylguanine-DNA Alkyltransferase Using Interstrand Cross-Linked DNA

Francis P. McManus,[‡] Amardeep Khaira,[‡] Anne M. Noronha,[‡] and Christopher J. Wilds*[,‡]

[‡]Department of Chemistry and Biochemistry, Concordia University, 7141 Sherbrooke St. West, Montréal, QC, Canada H4B 1R6

Supporting Information

ABSTRACT: O^6-alkylguanine-DNA alkyltransferases (AGT) are responsible for the removal of alkylation at both the O^6 atom of guanine and O^4 atom of thymine. AGT homologues show vast substrate differences with respect to the size of the adduct and which alkylated atoms they can restore. The human AGT (hAGT) has poor capabilities for removal of methylation at the O^4 atom of thymidine, which is not the case in most homologues. No structural data are available to explain this poor hAGT repair. We prepared and characterized O^6G-butylene-O^4T (XLGT4) and O^6G-heptylene-O^4T (XLGT7) interstrand cross-linked (ICL) DNA as probes for hAGT and the *Escherichia coli* homologues, OGT and Ada-C, for the formation of DNA-AGT covalent complexes. XLGT7 reacted only with hAGT and did so with a cross-linking efficiency of 25%, while XLGT4 was inert to all AGT tested. The hAGT mediated repair of XLGT7 occurred slowly, on the order of hours as opposed to the repair of O^6-methyl-2′-deoxyguanosine which requires seconds. Sodium dodecyl sulfate-polyacrylamide gel electrophoresis (SDS-PAGE) analysis of the repair reaction revealed the formation of a covalent complex with an observed migration in accordance with a DNA-AGT complex. The identity of this covalent complex, as determined by mass spectrometry, was composed of a heptamethylene bridge between the O^4 atom of thymidine (in an 11-mer DNA strand) to residue Cys145 of hAGT. This procedure can be applied to produce well-defined covalent complexes between AGT with DNA.

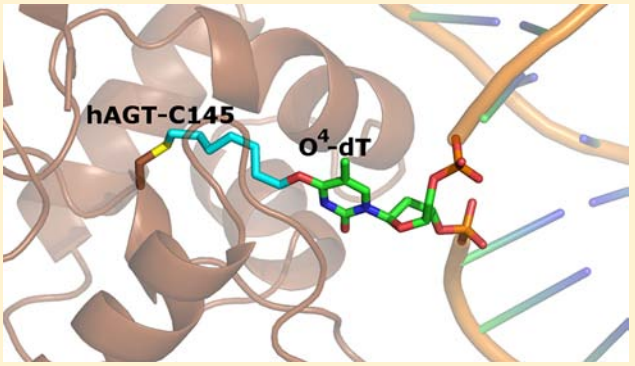

INTRODUCTION

Modified nucleic acids with novel properties have had a long-standing interest and application in the field of bioorganic chemistry.[1] One example of how these probes can be employed involves the formation of covalent complexes with proteins where weak binding was previously observed leading to a wide range of applications.[2−4]

Formation of covalent complexes for crystallographic purposes can be employed for various systems due to the control one can have on the nature of the chemical modification, which can be tailored to specific protein complexes.[5,6] For example, the structure of hAGT complexed with DNA has been determined with the aid of modified nucleic acids.[7,8] One of these structures, significant in enhancing our understanding of the mechanism of hAGT, contains a chemical cross-link formed between the hAGT active site and DNA containing the modified nucleoside N1,O^6-ethanoxanthosine.

AGT proteins, which are found in all kingdoms of life, are responsible for the repair of the mutagenic O^6-methylguanosine (O^6 MedG) and O^4-methylthymidine (O^4 MedT) lesions.[9−11] The mutagenicity of these lesions rise from the wobble base pair that these modified bases adopt with respect to their natural compliments. These wobble base pairs adversely affect the processivity of DNA polymerase during DNA replication. O^6 MedG adopts a nonwobble base pair with dT causing a GC to AT transition, while O^4 MedT adopts a nonwobble base pair with dG causing a TA to CG transition. These two modifications account for 8% of the total DNA damage caused by *N*-methyl-*N*-nitrosourea (MNU).[12] Endogenously, O^6 MedG is formed at a rate of 10−30 events daily by *S*-adenosylmethionine.[13]

The formation of O^6 MedG is detrimental to cells where the bioaccumulation of 6 650 O^6 MedG modifications in hAGT deficient tumor cells is sufficient to cause cell lethality.[14] Unlike O^6 MedG, O^4 MedT is affected by neither the levels of hAGT nor mismatch repair (MMR), which is why this lesion is more mutagenic in mammalian cells.[15,16] Processing of O^4 MedT in mammalian cells is believed to rely solely on the nucleotide excision repair (NER) pathway.[17]

hAGT and Ada-C, the most thoroughly characterized AGT proteins, repair alkylated DNA by flipping the damaged base out of the DNA duplex and into the active site where the alkyl group is transferred from the point of lesion to the active site-

Received: October 9, 2012
Revised: December 19, 2012
Published: January 24, 2013

 © 2013 American Chemical Society dx.doi.org/10.1021/bc300553u | *Bioconjugate Chem.* 2013, 24, 224−233

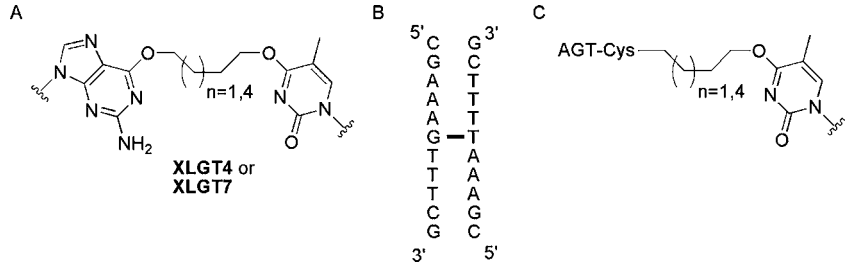

Figure 1. Structures of (A) the O^4-thymidine-alkylene-O^6-2′-deoxyguanosine cross-links, (B) oligonucleotides XLGT4 (n = 1) and XLGT7 (n = 4), and (C) AGT-DNA complex formed if XLGT4 and XLGT7 are repaired by AGT.

Cys residue.[18] Once alkylated, this suicide protein is degraded by the ubiquitin pathway in mammalian cells.[19] There are interesting differences in the ability of AGTs to process alkylation damage. For example, hAGT is unable to process O^4 MedT efficiently, unlike OGT and Ada-C.[20,21]

hAGT has also been employed in an elegant method to observe the movement of an hAGT fusion protein which reacts with O^6-benzylguanine derivatives.[22]

Previously, mimics of the ICL generated by 1,7-heptanediol dimethanesulfonate (hepsulfam) have been studied by our group.[23−25] Results from our previous work indicate hAGT, but not the *E. coli* homologues, can repair ICL that involve two O^6 atoms of 2′-deoxyguanosine that are directly opposed, in a 1,2 stagger, or in the more clinically relevant 1,3 staggered orientation. On the other hand, ICL DNA containing a heptamethylene linkage bridging the O^4 atoms of thymidine are inert to hAGT and the *E. coli* homologues.

In the current study, the preparation of an ICL containing an O^4-thymidine-alkylene-O^6-2′-deoxyguanosine cross-link is described. The approach to prepare this ICL involves the method described by Swann's group to prepare a "convertible" thymidine to introduce an alkyl chain with a terminal alcohol at the O^4 atom of thymidine followed by a Mitsunobu reaction at the O^6 atom of protected 2′-deoxyguanosine to form the alkylene linkage (Figure 1A).[26,27] hAGT, OGT, and Ada-C were expressed and purified to homogeneity to investigate their role in the repair of O^4-thymidine-alkylene-O^6-2′-deoxyguanosine ICL XLGT4 and XLGT7 (Figure 1B).

Aside from providing further insight into the substrate discrimination patterns of the various AGT, these ICL DNA have potential use for the preparation of site-specific covalently linked AGT-DNA adducts. The formation of AGT-oligonucleotide complexes between the various nucleobases has been shown to occur with 1,2-dibromoethane, attributed to the formation of an *S*-(2-bromoethyl) intermediate.[28] In our approach, repair by AGT at the O^6 atom of the modified 2′-deoxyguanosine by the active site Cys of AGT covalently links AGT to the O^4 atom of thymidine by an alkylene linker. The added facet of this approach is the ease with which the ICL linker can be varied allowing control over the length and chemical nature of the tether between the O^4 atom of thymidine and the active site of AGT (Figure 1c).

EXPERIMENTAL PROCEDURES

Materials. 5′-*O*-Dimethoxytrityl-N^2-phenoxyacetyl-2′-deoxyguanosine and *N*,*N*-diisopropylamino cyanoethyl phosphonamidic chloride were purchased from ChemGenes Inc. (Wilmington, MA). 5′-*O*-Dimethoxytrityl-2′-deoxyribonucleoside-3′-*O*-(β-cyanoethyl-*N*,*N*′-diisopropyl)phosphoramidites and protected 2′-deoxyribonucleoside-CPG (control pore glass) supports were purchased from Glen Research (Sterling, Virginia). All other chemicals and solvents were purchased from the Aldrich Chemical Co. (Milwaukee, WI) or EMD Chemicals Inc. (Gibbstown, NJ). Flash column chromatography was performed using silica gel 60 (230−400 mesh) obtained from Silicycle (Quebec City, QC). Thin layer chromatography (TLC) was performed using precoated TLC plates (Merck, Kieselgel 60 F_{254}, 0.25 mm) purchased from EMD Chemicals Inc. (Gibbstown, NJ). NMR spectra were recorded either on a Varian INOVA 300 MHz NMR spectrometer or on a Varian 500 MHz NMR spectrometer at room temperature. ^{1}H NMR spectra were recorded at a frequency of 300.0 MHz, and chemical shifts were reported in parts per million downfield from tetramethylsilane. ^{31}P NMR spectra (^{1}H decoupled) were recorded at a frequency of 202.3 MHz with H_3PO_4 used as an external standard. Ampicillin, isopropyl β-D-thiogalactopyranoside (IPTG), dithiothreitol (DTT), EASY-BLUE, Protein Stain, and most other biochemical reagents including polyacrylamide gel materials were purchased from Bioshop Canada Inc. (Burlington, ON). Ni-NTA Superflow Resin was purchased from Qiagen (Mississauga, ON). Complete, Mini, EDTA-free Protease Inhibitor Cocktail Tablets were obtained from Roche (Laval, QC) Nitrocellulose filters (0.20 μm) were obtained from Millipore. XL-10 Gold *E. coli* cells were obtained from Stratagene (Cedar Creek, TX). T4 polynucleotide kinase (PNK) and Unstained Protein Molecular Weight Marker were obtained from Fermentas (Burlington, ON). [γ-^{32}P]ATP was purchased from Amersham Canada Ltd. (Oakville, ON).

Chemical Synthesis of Modified Nucleosides. *1-{O^4-[3′-O-(t-Butyldimethylsilyl)-5′-O-(4,4′-dimethoxytrityl)-thymidinyl]}-4-{O^6-[3′-O-(t-butyldimethylsilyl)-5′-O-(4,4′-dimethoxytrityl)-N^2-phenoxyacetyl-2′-deoxyguanosinyl]}-butane (**1a**).* To 5′-*O*-dimethoxytrityl-3′-*O*-*t*-butyldimethylsilyl-N^2-(phenoxyacetyl)-2′-deoxyguanosine (0.150 g, 0.183 mmol) was added 5′-*O*-dimethoxytrityl-3′-*O*-*t*-butyldimethylsilyl-O^4-(hydroxybutyl)-thymidine (0.135 g, 0.185 mmol) and triphenylphosphine (0.208 g, 7.70 mmol) in dioxane (2 mL) followed by dropwise addition of diisopropyl azodicarboxylate (DIAD) (1.521 g, 7.52 mmol) at room temperature. After 30 min, the solvent was evaporated in vacuo, the crude product taken up in ethyl acetate (100 mL), and the solution washed with two portions of 3% sodium bicarbonate (2 × 100 mL). The organic layer was dried over sodium sulfate (4*g*) and concentrated to produce a yellow gum. The crude product was purified by flash column chromatography using a hexane/ethyl acetate (3:7) solvent system to afford 0.166 g (59%) of product as a colorless foam. R_f (SiO_2 TLC): 0.17 hexane/ethyl acetate (3:7).

^{1}H NMR (300 MHz, DMSO-d_6, ppm): 10.63 (s, 1H, NH), 8.45 (s, 1H, H8), 7.93 (s, 1H, H6), 7.46−6.79 (m, 31H, Ar),

dx.doi.org/10.1021/bc300553u | *Bioconjugate Chem.* 2013, 24, 224−233

6.45−6.40 (dd, 1H, H1′a, J = 6.3 Hz), 6.23−6.17 (dd, 1H, H1′b, J = 6.6), 5.06 (s, 2H, $PhOCH_2CO$), 4.74−4.70 (m, 1H, H3′a), 4.68−4.63 (t, 2H, CH_2-O^6), 4.50−4.46 (m, 1H, H3′b), 4.43−4.39 (m, 2H, CH_2-O^4), 3.95−3.90 (m, 2H, H4′a and H4′b), 3.78 (s, 6H, $O-CH_3$), 3.76 (s, 6H, $O-CH_3$), 3.42−3.22 (m, 4H, H5′a, H5″a, H5′b and H5″b), 3.04−2.97 (m, 1H, H2′a), 2.43−2.28 (m, 3H, H2″a, H2′b and H2″b), 2.03−1.90 (m, 4H, $O^4-CH_2-C\underline{H_2}-C\underline{H_2}-CH_2-O^6$), 1.64 (s, 3H, C5−$CH_3$), 0.83 (s, 18H, Si−$C(CH_3)_3$), 0.06 (s, 6H, Si−$CH_3$), 0.01 (s, 3H, Si−$CH_3$), 0.00 (s, 3H, Si−$CH_3$).

HRMS (ESI-MS) m/z calculated for $C_{86}H_{104}N_7O_{15}Si_2^+$ 1530.7129: found 1530.7087 $[M+H]^+$.

*1-{O^4-[3′-O-(t-Butyldimethylsilyl)-5′-O-(4,4′-dimethoxytrityl)-thymidinyl]}-7-{O^6-[3′-O-(t-butyldimethylsilyl)-5′-O-(4,4′-dimethoxytrityl)-N^2-phenoxyacetyl-2′-deoxyguanosinyl]}-heptane (**1b**).* To 5′-*O*-dimethoxytrityl-3′-*O*-*t*-butyldimethylsilyl-N^2-(phenoxyacetyl)-2′-deoxyguanosine (0.700 g, 0.851 mmol) was added 5′-*O*-dimethoxytrityl-3′-*O*-*t*-butyldimethylsilyl-O^4-(hydroxyheptyl) thymidine (0.600 g, 0.774 mmol) and triphenylphosphine (0.850 g, 3.25 mmol) in dioxane (8.46 mL) followed by dropwise addition of DIAD (0.720 g, 3.56 mmol) at room temperature. After 22 h, the solvent was evaporated in vacuo, the crude product taken up in ethyl acetate (100 mL) and the solution washed with two portions of 3% sodium bicarbonate (2 × 100 mL). The organic layer was dried over sodium sulfate (4*g*) and concentrated to produce a yellow gum. The crude product was purified by flash column chromatography using a hexane/ethyl acetate (1:1 → 4:6) solvent system to afford 0.77 g (70%) of product as a colorless foam. R_f (SiO_2 TLC): 0.33 hexane/ethyl acetate (4:6).

^{1}H NMR (300 MHz, $CDCl_3$, ppm): 8.72 (s,1H, NH), 8.10 (s, 1H, H8), 8.00 (s, 1H, H6), 7.50−6.84 (m, 31H, Ar), 6.52−6.48 (dd, 1H, H1′a, J = 6.6 Hz), 6.43−6.39 (dd, 1H, H1′b, J = 6.0 Hz), 4.86 (s, 2H, $PhOCH_2CO$), 4.68−4.64 (m, 2H, CH_2-O^6), 4.58−4.52 (m, 1H, H3′a), 4.46−4.41 (t, 2H, CH_2-O^4), 4.19−4.16 (m, 1H, H3′b), 4.05−4.01 (m, 2H, H4′a and H4′b), 3.86 (s, 6H, $O-CH_3$), 3.84 (s, 6H, $O-CH_3$), 3.60−3.31 (m, 4H, H5′a, H5″a, H5′b and H5″b), 2.82−2.73 (m, 1H, H2′a), 2.61−2.48 (m, 2H, H2″a and H2′b), 2.32−2.24 (m, 1H, H2″b), 2.00−1.95 (m, 2H, R−$\underline{CH_2}-CH_2-O^6$), 1.85−1.80 (m, 2H, R−$\underline{CH_2}-CH_2-O^4$), 1.66 (s, 3H, C5−$CH_3$), 1.58 (m, 2H, R−$\underline{CH_2}-CH_2-CH_2-O^6$), 1.50 (m, 4H, R−$\underline{CH_2}-\underline{CH_2}-CH_2-CH_2-O^4$), 0.93 (s, 9H, Si−$C(CH_3)_3$), 0.88 (s, 9H, Si−$C(CH_3)_3$), 0.12 (s, 3H, Si−$CH_3$), 0.07 (s, 3H, Si−$CH_3$), 0.00 (s, 6H, Si−$CH_3$).

HRMS (ESI-MS) m/z calculated for $C_{89}H_{110}N_7O_{15}Si_2^+$ 1572.7598: found 1572.7592 $[M+H]^+$.

*1-{O^4-[5′-O-(4,4′-Dimethoxytrityl)-thymidinyl]}-4-{O^6-[5′-O-(4,4′-dimethoxytrityl)-N^2-phenoxyacetyl-2′-deoxyguanosinyl]}-butane (**2a**).* To compound **1a** (0.150 g, 0.10 mmol) was added tetra-*n*-butylammonium fluoride (TBAF) (1 M in tetrahydrofuran (THF)) (0.059 g, 0.21 mmol) in THF (1 mL). After 30 min, the solvent was evaporated in vacuo and the crude product taken up in ethyl acetate (50 mL). The solution was washed with three portions of sodium bicarbonate (3 × 50 mL) followed by two back-extractions of the sodium bicarbonate washes with ethyl acetate (2 × 25 mL). The organic layer was dried over sodium sulfate (4*g*), evaporated in vacuo, and purified by flash column chromatography using an ethyl acetate/methanol (95:5) solvent system to afford 0.083 g (64%) of product as a colorless foam. R_f (SiO_2 TLC): 0.14 ethyl acetate/methanol (95:5).

^{1}H NMR (300 MHz, DMSO-d_6, ppm) (Figure S1): 10.60 (s, 1H, NH), 8.36 (s, 1H, H8), 7.81 (s, 1H, H6), 7.42−6.71 (m, 31H, Ar), 6.43−6.38 (dd, 1H, H1′a, J = 6.3 Hz), 6.22−6.17 (dd, 1H, H1′b, J = 6.3), 5.36−5.33 (m, 2H, OHa and OHb), 5.04 (s, 2H, $PhOCH_2CO$), 4.63−4.58 (t, 2H, CH_2-O^6), 4.53−4.49 (m, 1H, H3′a), 4.39−4.34(m, 3H, $C\underline{H_2}-O^4$ and H3′b), 4.02−3.95 (m, 2H, H4′a and H4′b), 3.74 (s, 6H, $O-CH_3$), 3.72 (s, 3H, $O-CH_3$), 3.71 (s, 3H, $O-CH_3$), 3.32−3.08 (m, 4H, H5′a, H5′b, H5″a and H5″b), 2.94−2.84 (m, 1H, H2′a), 2.42−2.12 (m, 3H, H2″a, H2′b and H2″b), 1.96−1.89 (m, 4H, $O^4-CH_2-C\underline{H_2}-CH_2-CH_2-O^6$).

HRMS (ESI-MS) m/z calculated for $C_{74}H_{76}N_7O_{15}^+$ 1302.5399: found 1302.5392 $[M+H]^+$.

*1-{O^4-[5′-O-(4,4′-Dimethoxytrityl)-thymidinyl]}-7-{O^6-[5′-O-(4,4′-dimethoxytrityl)-N^2-phenoxyacetyl-2′-deoxyguanosinyl]}-heptane (**2b**).* To compound **1b** (0.760g, 0.480 mmol) was added TBAF (1 M in THF) (0.282 g, 1.01 mmol) in THF (3 mL). After 30 min, the solvent was evaporated in vacuo and the crude product taken up in ethyl acetate (50 mL). The solution was washed with three portions of sodium bicarbonate (3 × 75 mL) followed by two back-extractions of the sodium bicarbonate washes with ethyl acetate (2 × 25 mL). The organic layer was dried over sodium sulfate (4*g*), evaporated in vacuo, and purified by flash column chromatography using an ethyl acetate/methanol (199:1 → 19:1) solvent system to afford 0.620 g (95%) of product as a colorless foam. R_f (SiO_2 TLC): 0.20 ethyl acetate/methanol (49:1).

^{1}H NMR (300 MHz, $CDCl_3$, ppm) (Figure S2): 8.79 (s, 1H, NH), 8.02 (s, 1H, H8), 8.85 (s, 1H, H6), 7.43−6.78 (m, 31H, Ar), 6.59−6.55 (dd, 1H, H1′a, J = 6.6 Hz), 6.44−6.37 (dd, 1H, H1′b, J = 6.3 Hz), 4.83 (m, 1H, OHa), 4.72 (s, 2H, $PhOCH_2CO$), 4.61−4.57 (m, 3H, CH_2-O^6 and H3′a), 4.39−4.35 (t, 2H, CH_2-O^4), 4.22−4.18 (m, 1H, H3′b), 4.16−4.11 (m, 2H, H4′a and H4′b), 3.80 (s, 6H, $O-CH_3$), 3.77 (s, 6H, $O-CH_3$), 3.51−3.33 (m, 4H, H5′a, H5″a, H5′b and H5″b), 2.99 (m, 1H, OHb), 2.82−2.76 (m, 1H, H2′a), 2.67−2.59 (m, 2H, H2″a and H2′b), 2.32−2.23 (m, 1H, H2″b), 1.93−1.86 (m, 2H, R−$\underline{CH_2}-CH_2-O^6$), 1.76−1.70 (m, 5H, R−$\underline{CH_2}-CH_2-O^4$ and C5-CH_3),1.58−1.44 (m, 6H, $O^4-CH_2-CH_2-\underline{CH_2}-\underline{CH_2}-\underline{CH_2}-CH_2-CH_2-O^6$).

HRMS (ESI-MS) m/z calculated for $C_{77}H_{82}N_7O_{15}^+$ 1344.5869: found 1344.5861 $[M+H]^+$.

*1-{O^4-[3′-O-(β-cyanoethyl-N,N′-diisopropyl)-5′-O-(4,4′-dimethoxytrityl)-thymidinyl]}-4-{O^6-[3′-O-(β-cyanoethyl-N,N′-diisopropyl)-5′-O-(4,4′-dimethoxytrityl)-N^2-phenoxyacetyl-2′-deoxyguanosinyl]}-butane (**3a**).* **2a** (0.200 g, 0.154 mmol) and diisopropylethylamine (0.060 g, 0.461 mmol) were dissolved in THF (1.5 mL). Then, *N*,*N*-diisopropylaminocyanoethylphosphonamidic chloride (0.091 g, 0.383 mmol) was added dropwise and the reaction allowed to stir at room temperature for 30 min. This was followed by two subsequent additions of diisopropylethylamine (2 × 0.012 g, 0.091 mmol) and *N*,*N*-diisopropylaminocyanoethylphosphonamidic chloride (2 × 0.019 g, 0.081 mmol) with 1 h intervals. Upon completion, the solvent was evaporated in vacuo, the crude product taken up in ethyl acetate (25 mL), and the solution washed with 3% sodium bicarbonate (25 mL) and brine (50 mL). The organic layer was dried over sodium sulfate, decanted, and evaporated. The product, a colorless powder, was precipitated from hexanes (0.221 g, 85%). R_f (SiO_2 TLC): 0.56, 0.61, 0.66, 0.73 ethyl acetate.

^{31}P NMR (202.3 MHz, d_6-acetone, ppm) (Figure S3): 153.61, 153.41, 153.40, 153.23.

dx.doi.org/10.1021/bc300553u | *Bioconjugate Chem.* 2013, 24, 224−233

HRMS (ESI-MS) m/z calculated for $C_{92}H_{110}N_{11}O_{17}P_2^+$ 1702.7556: found 1702.7557 $[M+H]^+$.

*1-{O^4-[3′-O-(β-cyanoethyl-N,N′-diisopropyl)-5′-O-(4,4′-dimethoxytrityl)-thymidinyl]}-7-{O^6-[3′-O-(β-cyanoethyl-N,N′-diisopropyl)-5′-O-(4,4′-dimethoxytrityl)-N^2-phenoxyacetyl-2′-deoxyguanosinyl]}-heptane (**3b**).* **2b** (0.200 g, 0.149 mmol) and diisopropylethylamine (0.058 g, 0.446 mmol) were dissolved in THF (1.5 mL). Then, *N,N*-diisopropylaminocyanoethylphosphonamidic chloride (0.088 g, 0.372 mmol) was added and the reaction allowed to stir at room temperature for 30 min. This was followed by two subsequent additions of diisopropylethylamine (2 × 0.012 g, 0.091 mmol) and *N,N*-diisopropylaminocyanoethylphosphonamidic chloride (2 × 0.019 g, 0.081 mmol) with 1 h intervals. Upon completion, the solvent was evaporated in vacuo, the crude product taken up in ethyl acetate (25 mL), and the solution washed with 3% sodium bicarbonate (25 mL) and brine (50 mL). The organic layer was dried over sodium sulfate, decanted, and evaporated. The product, a colorless powder, was precipitated from hexanes (0.218 g, 84%). R_f (SiO_2 TLC): 0.50, 0.58, 0.67, 0.75 ethyl acetate.

^{31}P NMR (202.3 MHz, d_6-acetone, ppm) (Figure S4): 153.60, 153.40, 153.39, 153.22.

HRMS (ESI-MS) m/z calculated for $C_{95}H_{116}N_{11}O_{17}P_2^+$ 1745.8032: found 1745.8059 $[M+H]^+$.

Solid-Phase Synthesis of XLGT4 and XLGT7. DNA duplexes XLGT4 and XLGT7 were assembled using an Applied Biosystems model 3400 synthesizer on a 1 μmol scale employing β-cyanoethylphosphoramidite cycles supplied by the manufacturer with certain modifications to coupling times as indicated below.

Commercially available fast deprotecting 3′-*O*-2′deoxynucleoside phosphoramidites were dissolved in anhydrous acetonitrile at a concentration of 0.1 M and the modified bis-3′-*O*-2′-deoxyphosphoramidites (**3a** and **3b**) at 0.05 M. Assembly of sequences began with detritylation (3% trichloroacetic acid (TCA) in CH_2Cl_2), followed by phosphoramidite coupling: commercial 3′-*O*-2′-deoxyphosphoramidites (2 min) and modified bis-phosphoramidite (**3a** and **3b**) (30 min); capping was performed with phenoxyacetic anhydride/pyridine/tetrahydrofuran (1:1:8, v/v/v; solution A) and 1-methyl-1*H*-imidazole/tetrahydrofuran (16:84 w/v; solution B) and oxidation (0.02 M iodine in tetrahydrofuran/water/pyridine 2.5:2:1) which followed every coupling. Final removal of trityl groups was carried out by the synthesizer to yield the final oligonucleotide on the solid support.

Due to the presence of an O^4-alkyl thymidine adduct, modifications to the standard deprotection protocol were employed. Deprotection of the oligonucleotide was achieved by incubating the CPG in 500 μL of 10% 1,8-diazabicyclo[5.4.0]-undec-7-ene (DBU) in ethanol for 3 days in the dark at room temperature.

XLGT4 and XLGT7 were purified from preterminated products by 20% 7 M urea denaturing polyacrylamide gels (19:1) using 1× TBE [89 mM Tris-HCl, 89 mM boric acid, 2 mM EDTA (pH 8.0)] as running buffer to remove any residual DBU. Prior to gel separation, 25 O.D. of DNA was lyophilized and resuspended in 100 μL of formamide. After electrophoresis, the desired DNA bands, as observed by UV shadowing, were excised from the gel and submerged overnight in 0.1 M sodium acetate. The extracted DNA was subsequently desalted using a C-18 SEP PAK cartridge (Waters Inc.).

Electrospray Ionization-Mass Spectrometry (ESI-MS) of Small Molecules and DNA. ESI-MS of XLGT4 and XLGT7 (Figures S5 and S6) were conducted at the Concordia University Centre for Biological Applications of Mass Spectrometry using a Micromass Q-tof2 mass spectrometer (Waters) equipped with a nanospray ion source. The mass spectrometer was operated in full scan, negative ion detection mode. ESI mass spectra for small molecules were recorded on a LTQ Orbitrap Velos-ETD (Thermo Scientific) in positive ion mode in acetonitrile.

Exonuclease Digestion. XLGT4 and XLGT7 (0.1 A_{260} units) were analyzed by exonuclease digestion (snake venom phosphodiesterase, 0.28 units; and calf intestinal phosphatase, 5 units, in 10 mM Tris-HCl, pH 8.1, and 2 mM magnesium chloride) for 4 days at 37 °C. Analysis of the resulting nucleoside mixtures were performed by reversed phase HPLC on a Symmetry C-18 5 μm column (0.46 × 15 cm). A linear gradient of 0−70% buffer B over 30 min was used to elute the various species (buffer A, 50 mM sodium phosphate, pH 5.8, 2% acetonitrile; and buffer B, 50 mM sodium phosphate, pH 5.8, 50% acetonitrile). The retention times of the eluted peaks (Figures S7 and S8) were compared to the standard nucleotides which eluted at the following times: dC (4.7 min), dG (7.5 min), dT (8.1 min), dA (8.9 min), O^6G-butylene-O^4T (18.4 min), and O^6G-heptylene-O^4T (25.3 min). The ratio of nucleosides was determined based on known extinction coefficients, aside from the cross-linked nucleosides where an extinction coefficient of 6200 M^{-1} cm^{-1} was used corresponding to the sum of the extinction coefficients of O^4 MedT and O^6 MedG (Table S1).

UV Thermal Denaturation Studies of DNA Duplexes. The molar extinction coefficients for XLGT4 and XLGT7 were determined using the nearest-neighbor method (M^{-1} cm^{-1}) assuming a central G-C match. On the basis of these extinction coefficients, the control DNA (having a G-C match instead of the ICL), XLGT4 and XLGT7 were lyophilized to dryness and reconstituted in 1 mL of 90 mM sodium chloride, 10 mM sodium phosphate, and 1 mM EDTA buffer (pH 7.0) at a final concentration of 3 μM. Prior to use, the samples were subjected to heating at 90 °C for 10 min and slowly cooled back to room temperature and finally stored at 4 °C overnight. The denaturation profiles were obtained by heating the samples at a rate of 0.5 °C min^{-1} while monitoring the absorbance at 260 nm using a Varian CARY model 3E spectrophotometer fitted with a six-sample thermostatted cell block and a temperature controller. Data processing was performed as described by Puglisi and Tinoco.[29]

Circular Dichroism (CD) Spectroscopy of DNA Duplexes. Circular dichroism signatures were obtained on a Jasco J-815 spectropolarimeter equipped with a Julaba F25 circulating bath using the samples prepared for UV thermal denaturation studies. The spectra were the average of 5 scans taken at a rate of 20 nm min^{-1}, with a bandwidth of 1 nm and sampling wavelength of 0.2 nm in a fused quartz cells (Starna 29-Q-10). Scans were performed between 320 and 220 nm at 10 °C. The molar ellipticity $[\phi]$ was obtained from the relation $\phi = \varepsilon/Cl$, where ε is the relative ellipticity (mdeg), C is the molar concentration of the DNA duplex (mol/L), and l is the path length in cm.

Protein Preparation. All AGT homologues were expressed under the promoter of the pQE30 vector in XL-10 Gold *E. coli* cells. The C145S hAGT variant was designed as described previously using site-directed mutagenesis.[24] The XL-10 Gold

host bacteria were grown in 1 L of LB broth + 100 μg/mL ampicillin until an OD_{600} = 0.6 was reached. After the addition of IPTG, at a final concentration of 0.3 mM, the cells were incubated at 37 °C for an additional 4 h. The cells were centrifuged at 6000*g* at 4 °C for 20 min and resuspended in lysis buffer [20 mM Tris-HCl (pH 8.0), 250 mM NaCl, and 20 mM β-mercaptoethanol supplemented with Complete, Mini, EDTA-free Protease Inhibitor Cocktail Tablets] at a final density of 1 g wet pellet per 5 mL of buffer. The cells were lysed by French press and the solution clarified by centrifuging at 17 000*g* for 45 min at 4 °C. The supernatant was applied to Ni-NTA column and washed with lysis buffer supplemented with 20 mM imidazole and the 6×His-tagged AGT proteins eluted with lysis buffer supplemented with 200 mM imidazole. The pooled fractions were dialyzed against storage buffer [50 mM Tris-HCl (pH 7.6), 250 mM NaCl, 20 mM β-mercaptoethanol, and 0.1 mM EDTA] in 8000 Da cutoff dialysis tubing. Ten milligrams of hAGT and OGT were obtained per liter of culture and 50 mg of Ada-C was obtained for the same volume.

Repair Assay. DNA substrates were labeled at the 5′ position using ^{32}P-ATP as previously described.[24] The labeling solution consisting of 200 pmol of dsDNA, 1 μL [γ-^{32}P]ATP (10 μCi/μL), and 5 units of T4 PNK in 10 μL of 1× PNK buffer was incubated at 37 °C for 1 h. The reactions were terminated by boiling the samples for 10 min and slowly cooling back to room temperature, the samples stored at 4 °C overnight and diluted 10-fold in Activity Buffer [10 mM Tris-HCl (pH 7.6), 100 mM NaCl and 1 mM DTT] prior to use.

Repair studies of XLGT4 and XLGT7 were performed by incubating 2 pmol of DNA and 60 pmol of AGT in a total volume of 15 μL made up of Activity Buffer and allowed to react at 37 °C for the desired time.[23] Prior to gel loading, the reactions were terminated by adding 18.2 μL of stop reaction buffer [81 mM Tris-HCl, 81 mM boric acid, 1.8 mM EDTA, and 1% SDS (sodium dodecyl sulfate) (pH 8.0) in 80% formamide] and boiled for 5 min. The samples were analyzed by 17% 7 M urea denaturing polyacrylamide gel (19:1) run in 1× TBE [89 mM Tris-HCl, 89 mM boric acid, 2 mM EDTA (pH 8.0)] for 1.5 h at 700 V. The gels were exposed to a storage phosphor screen, the image captured on a Typhoon 9400 (GE Healthcare, Piscataway, NJ) and the radioactive counts quantified by ImageQuant (Amersham Biosciences).

Identification of XLGT7 Repair Product by SDS-PAGE. 600 pmol of hAGT was incubated with 625 pmol of XLGT7 in 15 μL of Activity Buffer for 5 h at 37 °C. The reaction was terminated by adding 10 μL of SDS Buffer [125 mM Tris-HCl (pH 7.6), 2% SDS, 30% glycerol and 7.5% 2-mercaptoethanol], boiling the sample for 5 min, and separated on a 15% SDS-PAGE. The gel was stained with EASY-BLUE Protein Stain as per the manufacturer's protocol.

Identification of XLGT7 Repair Product by ESI-MS. 4000 pmol of hAGT was incubated with 1200 pmol of XLGT7 in 100 μL of Activity Buffer for 3 h at 37 °C. Ten microlilters of the sample was loaded on a Spursil C-18 column (3 μm, 2.1 mm ×150 mm) using an Agilent 1200 Series LC system at a flow rate of 0.2 mL/min with the following gradient program: 0−5 min, hold at 5% B; 5−30 min, linear gradient from 5% B to 50% B; 30−40 min, linear gradient from 50% B to 90% B; 40−42 min, hold at 90% B; 42−50 min, linear gradient from 90% B to 5% B (buffer A, 0.1% formic acid in water and buffer B, 0.1% formic acid in acetonitrile). ESI-MS was conducted on a Micromass Q-Tof Ultima API with the following conditions: source voltage 3.5 kV, mass range of 700−1999 *m*/*z* in positive ion mode. The theoretical mass of the hAGT-DNA species was calculated to be either 25 303.6 Da if the repair event occurred at the modified 2′-deoxyguanosine (21876.2 Da (hAGT) + 96.2 Da (Linker) + 3331.2 Da (CGAAATTTTCG)) or 25 328.6 Da if the repair event occurred at the modified thymidine (21 876.2 Da (hAGT) + 96.2 Da (Linker) + 3356.2 Da (CGAAAGTTTCG)).

C145S hAGT Binding Studies. Binding reactions consisted of 0.5 nM dsDNA, increasing C145S hAGT ranging from 1 to 5 μM in a total volume of 20 μL of Binding Buffer [10 mM Tris-HCl (pH 7.6), 100 mM NaCl, 1 mM DTT, 10 μg mL^{-1} BSA, and 2.5% glycerol]. The samples were incubated for 30 min at room temperature and loaded on a 15% native polyacrylamide gel (75:1) containing 0.5× TBE. Electrophoresis was carried out using 0.5× TBE as running buffer at 21 °C with 250 V for 25 min. The gel was processed as described above for the repair assay.

Binding parameters for the AGT-DNA interaction were obtained from the electrophoretic mobility shift assays as described previously.[30] Binding of *n* moles of AGT protein [P] to a mole of DNA [D] is described by the equation: $nP + D \leftrightarrow P_nD$. Taking the logarithm yields: $\log([P_nD]/[D]) = n \log [P]_{free} + \log K_n$. Plotting of $\log [P_nD]/[P]$ as a function of $\log [P]$ produces a slope that represents the stoichiometry (*n*), and the K_n can be obtained from the relationship $K_n = 10^{-(y\text{-intercept})}$. The reported K_d (dissociation constant) was obtained by taking the *n*th root of K_n.

RESULTS

Substrate Preparation. The structures of XLGT4 and XLGT7 are shown in Figure 1. The O^6G-butylene-O^4T (**3a**) and O^6G-heptylene-O^4T (**3b**) cross-linked amidites were prepared as shown in Scheme 1 which began with the nucleoside adduct containing a tetra- or heptamethylene linker with a terminal alcohol which was prepared by reacting the appropriate dialcohol with 3′-*O*-(*tert*-butyldimethylsilyl)-5′-*O*-(4,4′-dimethoxytrityl)-O^4-triazolyl-thymidine.[25] The 3′ and 5′ bis-protected thymidine adducts were subsequently reacted with 5′-*O*-dimethoxytrityl-3′-*O*-*t*-butyldimethylsilyl-N^2-(phenoxyacetyl)-2′-deoxyguanosine via a Mitsunobu reaction to give the fully protected dimers **1a** and **1b**.[31] Desilylation of the dimers gave **2a** and **2b** and was followed by a phosphitylation reaction yielding the cross-linked bis-amidites **3a** and **3b**, which were employed for solid-phase synthesis. ^{31}P NMR signals at 153.61, 153.41, 153.40, and 153.23 ppm for **3a** and 153.60, 153.40, 153.39, and 153.22 ppm for **3b** confirmed the presence of both phosphoramidite groups. As a result of the asymmetry for the phosphitylated cross-linked nucleosides, four ^{31}P NMR signals were observed.

ESI-MS and Exonuclease Digestion of DNA. XLGT4 and XLGT7 were analyzed by mass spectrometry to ensure that the base modifications were present after the deprotection and purification steps (Figures S5 and S6). The observed masses were in agreement with calculated values.

XLGT4 and XLGT7 nucleoside compositions were confirmed by exonuclease digestion to their constituent nucleosides with a mixture of snake venom phosphodiesterase and calf intestinal phosphatase, then analyzed by C-18 reversed phase HPLC. The elution profiles are shown in Figures S7 and S8. The presence of modified nucleosides was established by the appearance of additional peaks, aside from the four standard nucleosides, on the HPLC chromatogram. The extracted ratios

Scheme 1[a]

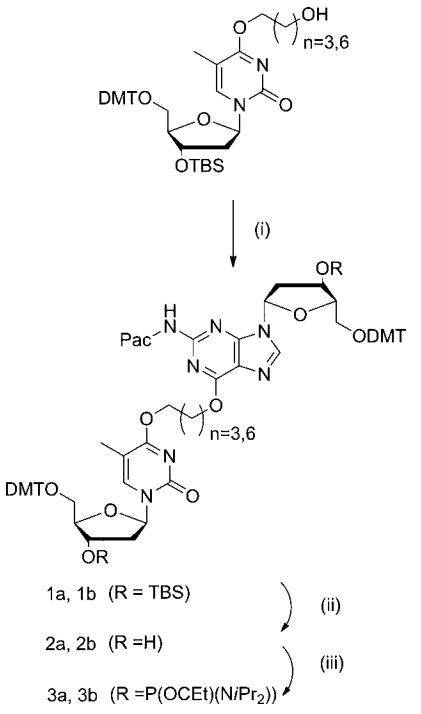

[a]Reagents and conditions: (i) 5′-*O*-dimethoxytrityl-3′-*O*-*t*-butyldimethylsilyl-N^2-(phenoxyacetyl)- 2′-deoxyguanosine, triphenylphosphine, DIAD, dioxane; (ii) tetrabutylammonium fluoride (1 M in THF), THF; (iii) *N*,*N*-diisopropylamino cyanoethyl phosphonamidic chloride, diisopropylethylamine, THF.

of the component 2′-deoxynucleosides were in good agreement with the theoretical compositions except for the lower than anticipated proportion of cross-linked modifications due to their assumed extinction coefficients, as illustrated in Table S1.

UV Thermal Denaturation Studies of DNA Duplexes. The stability of XLGT4 and XLGT7 containing duplexes were determined by UV thermal denaturing studies by monitoring OD_{260} at increasing temperatures, as illustrated in Figure 2.

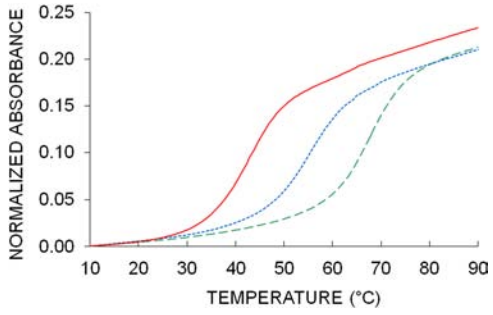

Figure 2. T_m curves of XLGT4, XLGT7, and control DNA duplexes. Control DNA (red), XLGT4 (green), and XLGT7 (blue).

Both modified duplexes displayed sigmoidal denaturation patterns comparable to the control duplex. The presence of the ICL stabilized the DNA duplex with the 4 methylene linker having a greater contribution than the 7 methylene linker. The melting temperatures for XLGT4, XLGT7, and the control (G-C pair instead of a G-T cross-link) were 68, 56, and 46 °C, respectively.

Circular Dichroism Spectroscopy of DNA Duplexes. The alkylene linkers present in XLGT4 and XLGT7 showed little effect on overall secondary structure as indicated by the characteristic B-form DNA signatures observed for all samples with positive signals centered around 275 nm, cross overs around 260 nm, and negative signals around 250 nm, as shown in Figure 3.[32,33] These results are in agreement with previously studied ICL DNA having central O^4-thymidine-alkylene-O^4-thymidine and O^6-2′-deoxyguanosine-alkylene-O^6-2′-deoxyguanosine mismatches showing classic B-form CD signatures.[25,34]

Repair Assay. Sixteen hour repair reactions with the various AGT and XLGT4 or XLGT7 were conducted to detect the total amount of repair by the different AGT homologues. The positive control XLGG7 (O^6-2′-deoxyguanosine-heptylene-O^6-2′-deoxyguanosine ICL) incubated with hAGT was used as a marker, since the various species produced by this reaction are known and aid in the identification of the various products formed in our assay, including two slowly migrating bands corresponding to AGT-DNA complexes that are believed to be either fully reduced or partially reduced by 2-mercaptoethanol.[24]

No appreciable repair was observed by any of the AGT tested with XLGT4 (data not shown). Repair of XLGT7, shown in Figure 4, was achieved only by hAGT, where 25% of

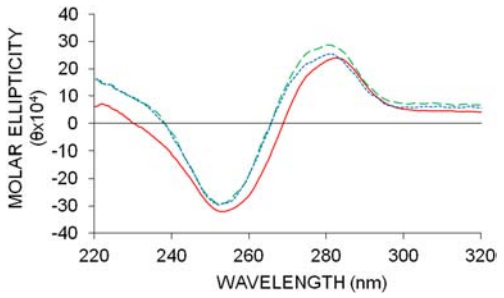

Figure 3. Far-UV circular dichroism spectra of XLGT4, XLGT7, and control DNA duplexes: Control DNA (red), XLGT4 (green), and XLGT7 (blue).

the starting material was converted to the AGT-DNA covalent complex. Moreover, the ratio of the released DNA strand and

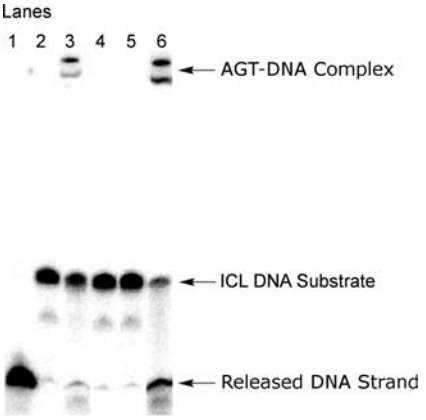

Figure 4. Denaturing PAGE gel illustrating the repair of XLGT7 by hAGT, Ada-C and OGT using 2 pmol of DNA and 60 pmol AGT at 37 °C for 16 h. Lane 1, Control DNA + hAGT; lane 2, XLGT7; lane 3, XLGT7 + hAGT; lane 4, XLGT7 + OGT; lane 5, XLGT7 + Ada-C; lane 6, XLGG7 + hAGT.

dx.doi.org/10.1021/bc300553u | *Bioconjugate Chem.* 2013, 24, 224−233

AGT-DNA complex was 1:1, suggesting hAGT only repaired one of the alkylated atoms involved in the cross-link. This hAGT repair activity was abolished by introducing the C145S mutation (data not shown).

The repair rate of XLGT7 and formation of the hAGT-DNA complex was monitored over the course of 3 h to obtain information on the kinetics of this reaction, as shown in Figure 5. The results indicate that the repair occurred slowly where

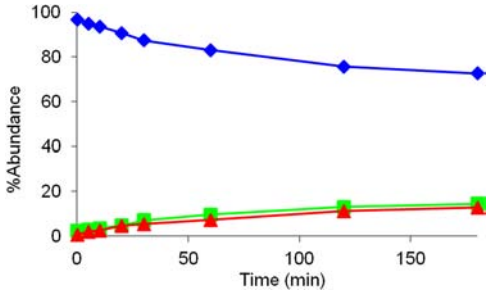

Figure 5. Time course repair of XLGT7 by hAGT. Substrate (♦), hAGT-DNA complex (▲), and released DNA strand (■).

only 13% of the AGT-DNA species is present after the three hour period. As was the case for the repair assay conducted overnight, the ratio of AGT-DNA complex to released DNA strand was 1:1.

Identification of XLGT7 repair product by SDS-PAGE and ESI-MS. Since the radioactivity-based repair assays only show the DNA species, SDS-PAGE was conducted on the hAGT mediated repair of XLGT7 to observe the various protein species formed. The SDS-PAGE shown in Figure 6

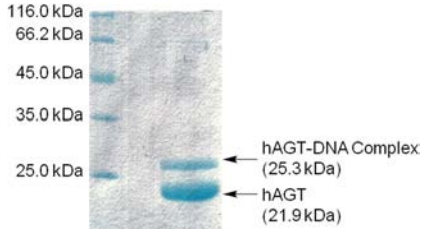

Figure 6. 15% SDS-PAGE of hAGT mediated repair of XLGT7. Repair of 625 pmol XLGT7 by 600 pmol hAGT for 5 h at 37 °C: unstained protein molecular weight marker (left); XLGT7 + hAGT reaction (right).

reveals the formation of a protein complex with a greater molecular weight than unmodified hAGT. On the basis of the results from Figures 4 and 6, we hypothesize that the new species corresponds to an hAGT-DNA covalent complex, which coincides with the calculated mass of (25.3 kDa).

The identity of the hAGT-DNA complex hypothesized from Figure 6 was determined using ESI-MS. Since the cross-link involves two different alkylated nucleotides that could potentially be repaired by hAGT, it was necessary to identify the hAGT-DNA species in order to establish the site of repair. Repair at either of the alkylation sites will yield an hAGT-DNA species of a different mass aiding in identification.

The ESI-MS spectrum of the hAGT mediated repair of XLGT7 is shown in Figure 7. Two major signals are observed in the deconvoluted spectrum. The first corresponds to the unalkylated form of hAGT and the second the hAGT-DNA covalent complex. On the basis of the observed and calculated masses, the hAGT-DNA complex occurs between the protein and the DNA strand alkylated at the O^4 atom of thymidine, indicating hAGT preferentially repairs the alkylated 2′-deoxyguanosine (Figure 8).

C145S hAGT Binding Studies. Binding assays were carried out to study the effect of the ICL on hAGT substrate discrimination in hopes of understanding the preferential repair observed for XLGT7 over XLGT4 (see Figure S9). Results presented in Table 1 indicate that hAGT binds both ICL DNA in a similar 2:1 (protein/DNA) stoichiometry, similar to the control DNA, suggesting the cross-links have no evident effect on the mode of hAGT binding.

The K_d values extracted from the EMSA suggest hAGT binds XLGT7 2-fold better than the control DNA and XLGT4, which are both bound in the low μM range.

■ DISCUSSION

Directly opposed O^6-2′-deoxyguanosine-alkylene-O^4-thymidine ICL were prepared using a combination of solution synthesis to create the cross-linked phosphoramidite and solid-phase synthesis to incorporate the cross-link into an oligonucleotide. The identities of the ICL DNA XLGT4 and XLGT7 were confirmed by ESI-MS and exonuclease digestion. The nucleoside ratios extracted from the digestion were in accordance with the theoretical composition of the oligonucleotide except for a lower than anticipated ratio of the cross-linked nucleosides. These deviations in ratios are attributed to the unknown extinction coefficient for these novel nucleosides where the sum of the extinction coefficients of O^4 MedT and O^6 MedG was used to get an estimate of the relative ratio of these modifications. The complimenting nature of the ESI-MS validates the presence of only one ICL modification per DNA molecule.

The presence of the cross-links increased the thermal stability of the DNA duplex, where the presence of a four methylene bridge had a greater stabilizing effect than the seven as observed by our UV thermal denaturation studies. The smaller increase in thermal stability brought upon by the larger ICL is believed to be due to a greater reduction in the enthalpy for the heptylene versus butylene linker containing DNA, which may be attributed to the disruption of the base pairs around the cross-linked site as a result of steric effects of the larger linker.[25] A comparable trend has been observed previously by our group for an O^4-thymidine-alkylene-O^4-thymidine mismatch where an increase in melting temperature (T_m) of 9 and 25 °C was observed over the control duplex for the heptylene and butylene linkages, respectively.[25] This also holds true for an O^6-2′-deoxyguanosine-alkylene-O^6-2′-deoxyguanosine mismatch in a similar oligonucleotide sequence with 12 and 24 °C increases in T_m for the heptylene and butylene linkages over our control DNA, respectively.[34] Indeed, the presence of an ICL, irrespective of the length, causes a reduction in the change of entropy upon denaturation of the duplex due to the organized nature of the unimolecular system. As previously observed, the contribution of the entropy factor overrides the negative enthalpic effect on the ICL system affording a more stable species.[35]

The control DNA, XLGT4, and XLGT7 all assumed a B-form structure as assessed by far-UV CD. These results are in accordance with previously studied ICL DNA having cross-links between the N^3 atoms of thymidine and the N^4 atoms of cytidine.[36,37] Moreover, NMR studies on ICL DNA containing an N^3-thymidine-butylene-N^3-thymidine cross-link revealed no

dx.doi.org/10.1021/bc300553u | Bioconjugate Chem. 2013, 24, 224−233

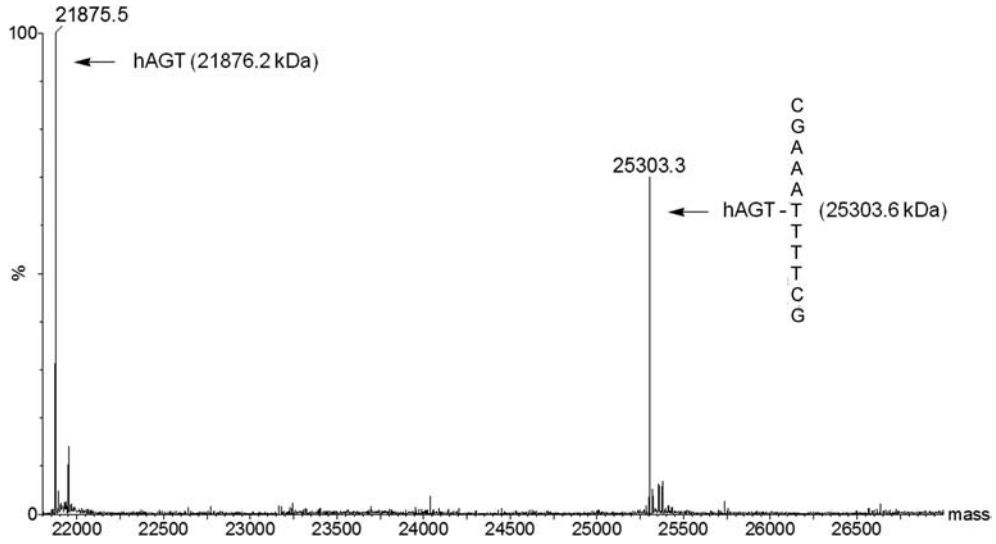

Figure 7. Identification of hAGT-DNA covalent complex by ESI-MS.

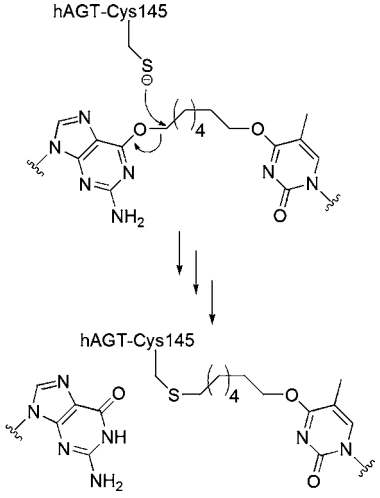

Figure 8. hAGT mediated repair of XLGT7 cross-link.

Table 1. K_d and Stoichiometry of Binding by hAGT to XLGT4, XLGT7, and Control Duplex

DNA duplex	K_d (μM)	stoichiometry
Control (G-C)	3.55 ± 0.14	2.03 ± 0.08
XLGT4	3.64 ± 0.20	1.99 ± 0.17
XLGT7	2.05 ± 0.05	1.97 ± 0.02

change in the overall B-form structure of the DNA but did show widening of the major groove without compromising the size of the minor groove.[38]

The conformation of the DNA probe might play a substantial role in hAGT repair. The repair of O^6-methyl-guanosine (O^6-methyl-riboG) in a DNA strand by hAGT is nonexistent as opposed to its natural substrate, O^6MedG which is efficiently processed by the protein.[39] On the basis of hAGT-DNA cocrystals, the lack of RNA repair by hAGT has been attributed to a potential steric clash between the 2′ hydroxyl of the modified ribonucleoside and the α-carbon of Gly131.[7] This only partially addresses the discriminatory pattern. Other nucleic acid properties may be responsible for this discerning trend. Notably, differences in the ribose and 2′-deoxyribose sugar puckers, affecting the overall secondary structure of nucleic acids, could play a part in poor RNA repair by hAGT. For this reason, the B-form structure of DNA may be primordial for AGT repair.

Our radioactivity-based repair assay revealed no repair of XLGT4 by any AGT tested. Lack of repair by OGT and Ada-C was anticipated based on previous work, which indicates that both proteins are inactive to ICL DNA.[23,25]

The absence of any appreciable repair of XLGT4 by hAGT was surprising considering its ability to repair O^6-2′-deoxyguanosine-butylene-O^6-2′-deoxyguanosine ICL (XLGG4) in a virtually identical sequence.[23,24] The difference in size between thymidine and guanosine may be responsible for the lack of XLGT4 repair as opposed to XLGG4. Replacing one 2′-deoxyguanosine by a thymidine reduces the linear distance between the anomeric carbons of the modified nucleosides by roughly 1 Å.

A molecular model generated by Fang et al. of hAGT in complex with XLGG7 suggests the preferential repair of longer cross-links by hAGT is brought upon by the shape of the hAGT active site in the DNA-bound conformation, which can be represented as a tunnel.[23] In effect, the larger the distance between the anomeric carbons of the modified nucleosides, the greater the ICL repair since the cross-linked nucleobases will sit at each end of the hAGT active site ″tunnel″. This allows the linker to lay in the ″tunnel″ while at the same time placing the α-carbon of the adduct in close proximity to the reactive Cys residue.

Local denaturation of the DNA duplex upon hAGT binding may be the cause for the extension of the cross-link, whereby separating the tethered nucleotides.[40] As eluded to in earlier studies based on the thermal denaturation results, the larger cross-link causes the disruption of the base pairs around the lesion itself generating a substrate that is already denatured around the point of alkylation prior to protein binding.

Repair of XLGT7 was achieved only by hAGT, as was anticipated based on the ″tunnel″ model. Increasing the length of the ICL allowed the nucleobases to span the distance of the hAGT active site, permitting repair to occur. Repair of XLGT7 by hAGT shown in lane 3 of Figure 4 suggests the formation of a species that corresponds to a AGT-DNA complex, based on the migration pattern of the XLGG7 control from lane 6, as well as a fully repaired DNA strand, which migrated similarly to

dx.doi.org/10.1021/bc300553u | Bioconjugate Chem. 2013, 24, 224−233

the control DNA in lane 1. The formation of the AGT-DNA complex and the release of the repaired strand in a 1:1 ratio implies that repair by hAGT only occurred at one site per DNA molecule. Repair of XLGT7 by hAGT required hours for completion as indicated by the time course assay shown in Figure 5. The C145S variant of hAGT was unable to repair XLGT7 identifying Cys145 as the reactive residue.

To overcome the limitations of the radioactivity-based assay, which only monitors the DNA species, an SDS-PAGE analysis of the reaction was performed to analyze the various proteinaceous materials formed. The absence of a protein band at 43.8 kDa, which would indicate an hAGT dimer linked by the seven methylene linker, supports the finding that hAGT only reacts at one location on XLGT7. A band just above the 25 kDa marker correlates to a covalent species migrating with a molecular weight corresponding to an AGT-DNA complex in a 1:1 ratio (roughly 25.3 kDa), which is in agreement with our radioactivity-based repair assay.

The identity of the covalent complex was determined by ESI-MS. The spectrum shown in Figure 7 displays some unreacted hAGT (21 875.5 Da) and a peak with a mass of 25 303.3 Da, corresponding to an hAGT-$(CH_2)_7$-CGAAAT<u>T</u>TTTCG molecule. The absence of a peak at 25 328.6 Da indicates hAGT reacts selectively at one location on the DNA duplex. To form this hAGT-$(CH_2)_7$-CGAAAT<u>T</u>TTTCG product, where the underlined nucleoside depicts the cross-linked position, hAGT must react on the modified CGAAA<u>G</u>TTTCG strand thereby releasing the repaired CGAAAGTTTCG oligonucleotide in the process. The absence of any formation of a covalent complex when reacting hAGT with the control DNA signifies the reactive moiety on the DNA as the O^6 atom of the cross-linked 2′-deoxyguanosine. The repair events of XLGT7 by hAGT have been summarized in Figure 8. These results are consistent with our previous results that demonstrate that hAGT can repair O^6-2′-deoxyguanosine-alkylene-O^6-2′-deoxyguanosine cross-links but is inert toward O^4-thymidine-alkylene-O^4-thymidine cross-links.[23−25]

The inability of hAGT to repair XLGT4 was not attributed to poor substrate binding as established from our EMSA results shown in Table 1. A 2-fold decrease in K_d observed for XLGT7 over XLGT4 and the control DNA is not substantial enough to support the repair trend. Also, the ICL had no effect on the binding stoichiometry of hAGT to the DNA. This is in agreement with the minor groove binding property of hAGT and the solution structure of similar ICL DNA showing the cross-link spanning the major groove without influencing the size of the minor groove.[7,38,41]

Using our approach, a well-defined hAGT-DNA covalent complex was generated covalently linking an O^4 alkylated thymidine via a seven methylene linker to hAGT. Unfortunately, the protein−DNA cross-linking reaction was limited to the human homologue where no complex was observed for Ada-C and OGT *E. coli* proteins. No complex was observed with the four methylene linker containing DNA XLGT4. The reason for this substrate discrimination by hAGT is not known, but we hypothesize that the longer cross-link found in XLGT7 allows for easier access to the point of lesion, since (1) the two modified nucleosides can be separated further apart due to the increased length of the tether and (2) the larger cross-link allows for substantial local destabilization of the DNA duplex at the point of repair granting easier access to hAGT.

We conclude that the use of ICL DNA as substrates for the formation of site-specific AGT-DNA covalent complexes is promising. Synthesis of these modified oligonucleotides is straightforward and allows great control over the length of the desired tether. As demonstrated herein, hAGT specifically reacts with the O^6 alkyated 2′-deoxyguanosine of the cross-link allowing the formation of defined covalent complexes that may find applications in experiments involving the labeling of hAGT.

■ ASSOCIATED CONTENT

Ⓢ Supporting Information

XLGT4 and XLGT7 characterization data and representative EMSA binding plots are available. This material is available free of charge via the Internet at http://pubs.acs.org.

■ AUTHOR INFORMATION

Corresponding Author

*Telephone: (514)-848-2424 ext. 5798. Fax: (514)-848-2868. E-mail: Chris.Wilds@concordia.ca.

Notes

The authors declare no competing financial interest.

■ ACKNOWLEDGMENTS

This research was supported by grants from the Natural Sciences and Engineering Research Council of Canada (NSERC), the Canada Foundation for Innovation (CFI), and the Canada Research Chair (CRC) program. F.P.M. is the recipient of postgraduate fellowships from the Groupe de Recherche Axé sur la Structure des Protéines (GRASP) and NSERC. Members of the group would like to thank Dr. Anthony E. Pegg for the plasmids encoding the wild-type Ada-C, OGT, and hAGT genes.

■ REFERENCES

(1) Egli, M., and Pallan, P. S. (2010) The many twists and turns of DNA: template, telomere, tool, and target. *Curr. Opin. Struct. Biol. 20*, 262−275.

(2) Corneillie, T. M., Whetstone, P. A., Lee, K. C., Wong, J. P., and Meares, C. F. (2004) Converting weak binders into infinite binders. *Bioconjugate Chem. 15*, 1389−1391.

(3) Niemeyer, C. M. (2002) The developments of semisynthetic DNA-protein conjugates. *Trends Biotechnol. 20*, 395−401.

(4) Niemeyer, C. M. (2010) Semisynthetic DNA-protein conjugates for biosensing and nanofabrication. *Angew. Chem., Int. Ed. Engl. 49*, 1200−1216.

(5) Staker, B. L., Hjerrild, K., Feese, M. D., Behnke, C. A., Burgin, A. B., Jr, and Stewart, L. (2002) The mechanism of topoisomerase I poisoning by a camptothecin analog. *Proc. Natl. Acad. Sci. U. S. A. 99*, 15387−15392.

(6) Golan, G., Zharkov, D. O., Grollman, A. P., Dodson, M. L., McCullough, A. K., Lloyd, R. S., and Shoham, G. (2006) Structure of T4 pyrimidine dimer glycosylase in a reduced imine covalent complex with abasic site-containing DNA. *J. Mol. Biol. 362*, 241−258.

(7) Daniels, D. S., Woo, T. T., Luu, K. X., Noll, D. M., Clarke, N. D., Pegg, A. E., and Tainer, J. A. (2004) DNA binding and nucleotide flipping by the human DNA repair protein AGT. *Nat. Struct. Mol. Biol. 11*, 714−720.

(8) Duguid, E. M., Rice, P. A., and He, C. (2005) The structure of the human AGT protein bound to DNA and its implications for damage detection. *J. Mol. Biol. 350*, 657−666.

(9) Spratt, T. E., and Levy, D. E. (1997) Structure of the hydrogen bonding complex of O6-methylguanine with cytosine and thymine during DNA replication. *Nucleic Acids Res. 25*, 3354−3361.

(10) Preston, B. D., Singer, B., and Loeb, L. A. (1986) Mutagenic potential of O4-methylthymine in vivo determined by an enzymatic

approach to site-specific mutagenesis. *Proc. Natl. Acad. Sci. U. S. A. 83*, 8501−8505.
(11) Pegg, A. E. (2000) Repair of O(6)-alkylguanine by alkyltransferases. *Mutat. Res. 462*, 83−100.
(12) Kleibl, K. (2002) Molecular mechanisms of adaptive response to alkylating agents in Escherichia coli and some remarks on O(6)-methylguanine DNA-methyltransferase in other organisms. *Mutat. Res. 512*, 67−84.
(13) Rydberg, B., and Lindahl, T. (1982) Nonenzymatic methylation of DNA by the intracellular methyl group donor S-adenosyl-L-methionine is a potentially mutagenic reaction. *EMBO J. 1*, 211−216.
(14) Rasouli-Nia, A., Sibghat-Ullah, Mirzayans, R., Paterson, M. C., and Day, R. S., 3rd. (1994) On the quantitative relationship between O6-methylguanine residues in genomic DNA and production of sister-chromatid exchanges, mutations and lethal events in a mer- human tumor cell line. *Mutat. Res. 314*, 99−113.
(15) Pauly, G. T., and Moschel, R. C. (2001) Mutagenesis by O(6)-methyl-, O(6)-ethyl-, and O(6)-benzylguanine and O(4)-methylthymine in human cells: Effects of O(6)-alkylguanine-DNA alkyltransferase and mismatch repair. *Chem. Res. Toxicol. 14*, 894−900.
(16) Altshuler, K. B., Hodes, C. S., and Essigmann, J. M. (1996) Intrachromosomal probes for mutagenesis by alkylated DNA bases replicated in mammalian cells: A comparison of the mutagenicities of O4-methylthymine and O6-methylguanine in cells with different DNA repair backgrounds. *Chem. Res. Toxicol. 9*, 980−987.
(17) Klein, J. C., Bleeker, M. J., Roelen, H. C., Rafferty, J. A., Margison, G. P., Brugghe, H. F., et al. (1994) Role of nucleotide excision repair in processing of O4-alkylthymines in human cells. *J. Biol. Chem. 269*, 25521−25528.
(18) Verdemato, P. E., Brannigan, J. A., Damblon, C., Zuccotto, F., Moody, P. C., and Lian, L. Y. (2000) DNA-binding mechanism of the Escherichia coli ada O(6)-alkylguanine-DNA alkyltransferase. *Nucleic Acids Res. 28*, 3710−3718.
(19) Srivenugopal, K. S., Yuan, X. H., Friedman, H. S., and Ali-Osman, F. (1996) Ubiquitination-dependent proteolysis of O6-methylguanine-DNA methyltransferase in human and murine tumor cells following inactivation with O6-benzylguanine or 1,3-bis(2-chloroethyl)-1-nitrosourea. *Biochemistry 35*, 1328−1334.
(20) Sassanfar, M., Dosanjh, M. K., Essigmann, J. M., and Samson, L. (1991) Relative efficiencies of the bacterial, yeast, and human DNA methyltransferases for the repair of O6-methylguanine and O4-methylthymine. suggestive evidence for O4-methylthymine repair by eukaryotic methyltransferases. *J. Biol. Chem. 266*, 2767−2771.
(21) Zak, P., Kleibl, K., and Laval, F. (1994) Repair of O6-methylguanine and O4-methylthymine by the human and rat O6-methylguanine-DNA methyltransferases. *J. Biol. Chem. 269*, 730−733.
(22) Keppler, A., Gendreizig, S., Gronemeyer, T., Pick, H., Vogel, H., and Johnsson, K. (2003) A general method for the covalent labeling of fusion proteins with small molecules in vivo. *Nat. Biotechnol. 21*, 86−89.
(23) Fang, Q., Noronha, A. M., Murphy, S. P., Wilds, C. J., Tubbs, J. L., Tainer, J. A., et al. (2008) Repair of O6-G-alkyl-O6-G interstrand cross-links by human O6-alkylguanine-DNA alkyltransferase. *Biochemistry 47*, 10892−10903.
(24) McManus, F. P., Fang, Q., Booth, J. D., Noronha, A. M., Pegg, A. E., and Wilds, C. J. (2010) Synthesis and characterization of an O(6)-2′-deoxyguanosine-alkyl-O(6)-2′-deoxyguanosine interstrand cross-link in a 5′-GNC motif and repair by human O(6)-alkylguanine-DNA alkyltransferase. *Org. Biomol. Chem. 8*, 4414−4426.
(25) McManus, F. P., O'Flaherty, D. K., Noronha, A. M., and Wilds, C. J. (2012) Preparation of O4-alkyl-2′-deoxythymidine cross-linked DNA to probe recognition and repair by O6-alkylguanine-DNA alkyltransferases. *Org. Biomol. Chem. 10*, 7078−7090.
(26) Xu, Y. Z., and Swann, P. F. (1990) A simple method for the solid phase synthesis of oligodeoxynucleotides containing O4-alkylthymine. *Nucleic Acids Res. 18*, 4061−4065.
(27) Shibata, T., Glynn, N., McMurry, T. B., McElhinney, R. S., Margison, G. P., and Williams, D. M. (2006) Novel synthesis of O6-alkylguanine containing oligodeoxyribonucleotides as substrates for the human DNA repair protein, O6-methylguanine DNA methyltransferase (MGMT). *Nucleic Acids Res. 34*, 1884−1891.
(28) Liu, L., Pegg, A. E., Williams, K. M., and Guengerich, F. P. (2002) Paradoxical enhancement of the toxicity of 1,2-dibromoethane by O6-alkylguanine-DNA alkyltransferase. *J. Biol. Chem. 277*, 37920−37928.
(29) Puglisi, J. D., and Tinoco, I., Jr. (1989) Absorbance melting curves of RNA. *Methods Enzymol. 180*, 304−325.
(30) Fried, M. G., Kanugula, S., Bromberg, J. L., and Pegg, A. E. (1996) DNA binding mechanism of O6-alkylguanine-DNA alkyltransferase: stoichiometry and effects of DNA base composition and secondary structure on complex stability. *Biochemistry 35*, 15295−15301.
(31) Mitsunobu, O. (1981) The use of diethyl azodicarboxylate and triphenylphosphine in synthesis and transformation of natural products. *Synthesis 1*, 1−28.
(32) Johnson, W. C., Jr. (1985) Circular dichroism and its empirical application to biopolymers. *Methods Biochem. Anal. 31*, 61−163.
(33) Johnson, W. C., Jr. (1996) Circular Dichroism Instrumentation. In *Circular Dichroism and the Conformational Analysis of Biomolecules* (Fasman, G. D., Ed.) pp 433, Plenum Press, New York.
(34) Booth, J. D., Murphy, S. P., Noronha, A. M., and Wilds, C. J. (2008) Effect of linker length on DNA duplexes containing a mismatched O6-2′-deoxyguanosine-alkyl interstrand cross-link. *Nucleic Acids Symp. Ser. 52*, 431−432.
(35) Hofr, C., and Brabec, V. (2005) Thermal stability and energetics of 15-mer DNA duplex interstrand crosslinked by trans-diamminedichloroplatinum(II). *Biopolymers 77*, 222−229.
(36) Wilds, C. J., Noronha, A. M., Robidoux, S., and Miller, P. S. (2004) Mispair-aligned N3T-alkyl-N3T interstrand cross-linked DNA: synthesis and characterization of duplexes with interstrand cross-links of variable lengths. *J. Am. Chem. Soc. 126*, 9257−9265.
(37) Noronha, A. M., Noll, D. M., Wilds, C. J., and Miller, P. S. (2002) N(4)C-Ethyl-N(4)C cross-linked DNA: synthesis and characterization of duplexes with interstrand cross-links of different orientations. *Biochemistry 41*, 760−771.
(38) Webba da Silva, M. W., Bierbryer, R. G., Wilds, C. J., Noronha, A. M., Colvin, O. M., Miller, P. S., and Gamcsik, M. P. (2005) Intrastrand base-stacking buttresses widening of major groove in interstrand cross-linked B-DNA. *Bioorg. Med. Chem. 13*, 4580−4587.
(39) Pegg, A. E., Morimoto, K., and Dolan, M. E. (1988) Investigation of the specificity of O6-alkylguanine-DNA-alkyltransferase. *Chem. Biol. Interact. 65*, 275−281.
(40) Federwisch, M., Hassiepen, U., Bender, K., Rajewsky, M. F., and Wollmer, A. (1997) Recombinant human O6-alkylguanine-DNA alkyltransferase induces conformational change in bound DNA. *FEBS Lett. 407*, 333−336.
(41) Webba da Silva, M., Noronha, A. M., Noll, D. M., Miller, P. S., Colvin, O. M., and Gamcsik, M. P. (2002) Solution structure of a DNA duplex containing mispair-aligned N4C-ethyl-N4C interstrand cross-linked cytosines. *Biochemistry. 41*, 15181−15188.